



Proceedings of the

# PACIFIC OCEAN REMOTE SENSING CONFERENCE

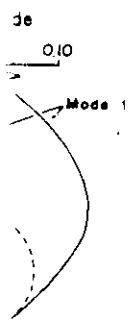
Melbourne, Australia

1-4 March 1994

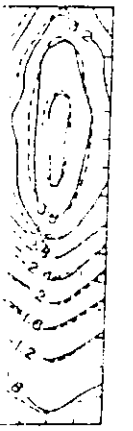


1985

Prasanna  
Kumar



Two modes and  
Perturbation.



271.55

17  
(12)

# ACOUSTIC PROPAGATIONS IN THE PRESENCE OF A SUBSURFACE COLD CORE EDDY IN THE BAY OF BENGAL - A CASE STUDY

S. Prasanna Kumar, G.S. Navelkar, T.V. Ramana Murty and  
C.S. Murty

National Institute of Oceanography, Dona Paula, Goa- 403 004,  
India.

## ABSTRACT

Acoustic characteristics of a cold core eddy, observed in the Bay of Bengal during southwest monsoon period is studied using CTD data along the western boundary. The presence of eddy brings about a reduction in the ambient sound speed by  $10 \text{ m.s}^{-1}$ . The depth of SOFAR channel axis which should have shown a deepening trend in this region remains constant under the influence of eddy. Ray tracing using a range-independent ray trace program showed that the arrivals are delayed by about 100-200 ms under the influence of the eddy. The acoustic intensity computed along the eigen ray passing through the eddy suffers an additional loss of the order of 20-25 dB. The simulated travel time perturbations associated with the eddy was inverted using singular value decomposition. From the numerical experiments it was found that inversion carried out using 18 eigen rays with 9 layers adequately resolve the eddy profile using 9 eigen modes.

## INTRODUCTION

In a recent study, a cold core, subsurface eddy centered at  $17^{\circ}40'N$  and  $85^{\circ}19'E$ , in the northwestern Bay of Bengal, was reported (Babu et al., 1991) based on the CTD data collected onboard ORV Sagar Kanya during 21-29 July 1984 (Fig.1). The thermo-haline structure indicated that it was confined below the mixed layer between 50 and 300 m depth and had a diameter of about 200 km. A temperature drop of about  $5^{\circ}C$  was observed at the center of the eddy. The salinity distribution showed that under the influence of the eddy, the core of the High Salinity Water (of Persian Gulf and Red Sea origin) is lifted upto 150 m depth, which otherwise existed at about 200 m depth. The prevailing baroclinic instability at the interface

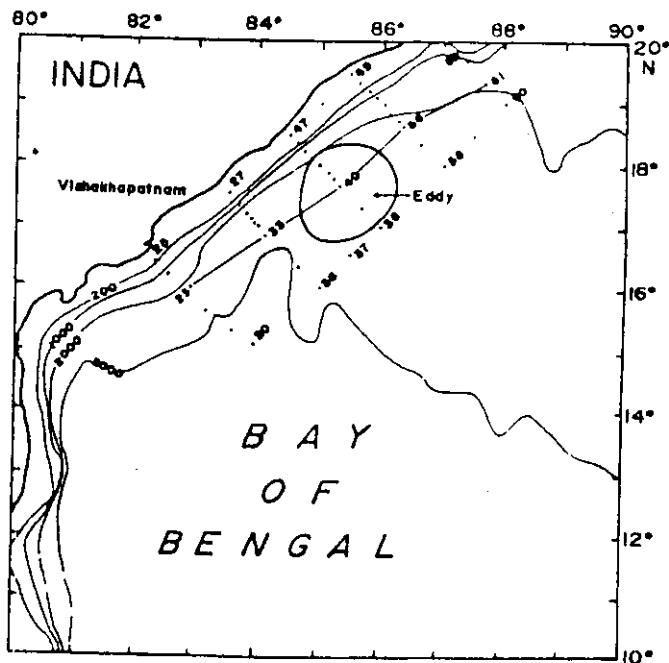


Fig.1 CTD stations location

of the opposing boundary currents along the shelf edge was suggested to be the generating mechanism of the observed eddy (Prasanna Kumar et al., 1992).

In this paper, we study the acoustic characteristics of this eddy and explore the possibility to reconstruct the acoustic profile of the eddy through generalized inverse from simulated travel time perturbations.

### SOUND SPEED STRUCTURE

In order to examine variability of acoustic field associated with the cold core eddy, sound speed structure across the eddy along two transect, shore parallel and shore normal, is presented (Fig.2). The signature of the subsurface eddy is clearly seen in both the sections by way of uplifting of isopleths. The maximum displacement of 150 m is associated with 1505  $m.s^{-1}$  isopleth at station 40 (Fig.2a). Thus the effect of cold core eddy is to reduce the ambient sound speed by about 10  $m.s^{-1}$ . Associated with this, the SOFAR channel also showed changes. Earlier studies in the Bay of Bengal (Prasanna Kumar et al., 1993) showed that the depth of SOFAR channel axis, in general, increases from southwest to northeast in the study region. However, it could be seen that (Fig.2a) in the present case though there is a general trend of deepening (from 1300 to 1800 m), the depth of the channel below the cold core eddy remained constant (1600 m). Accordingly, the sound speed at the channel axis below the eddy reduces by about 1.5  $m.s^{-1}$ . Since the signature of the eddy is

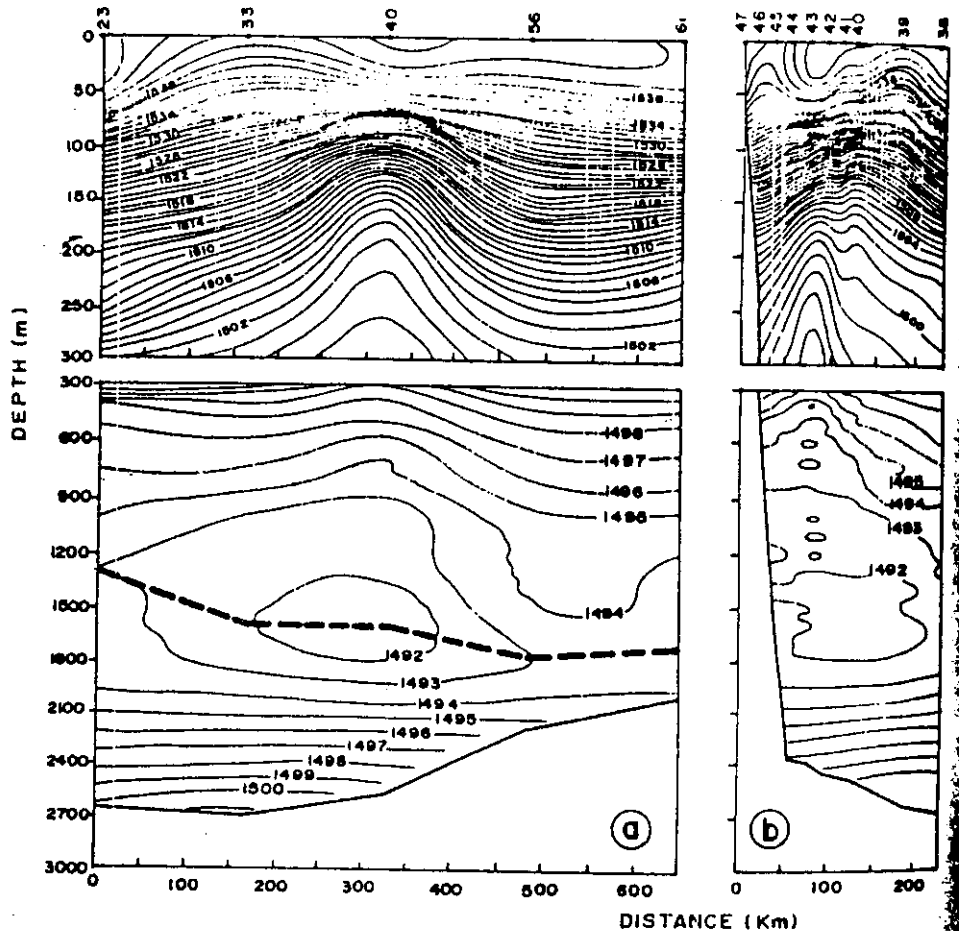


Fig.2 Sound speed structure across the eddy (a) parallel (b) normal to the coast --- indicate SOFAR axis depth.

Since the signature of the eddy is

strongest at station 40, sound speed profile at this station has been taken as the eddy profile for further computations.

### RAY ARRIVAL PATTERN

In order to understand the effect of cold core eddy on acoustic propagation, a range independent acoustic ray trace program is made use of (Ramana Murty et al., 1990). A mean sound speed profile is constructed from all the CTD data using the Chen and Millero (1977) formula. The ray tracing was carried out using the mean as well as the eddy profile for a range of 300 km with the source and the receiver at depths of 1600 m and 1500 m respectively.

The predicted arrival pattern (Fig.3) depicts the typical characteristics of the Bay of Bengal sound propagation: the early arrival cluster of near axial flat angle rays (+3 to -3); later arrivals of deep-turning rays followed by the weak latest arrivals of near-surface turning rays (RBR). This arrival pattern arises due to the weak acoustic wave guide nature of the Bay of Bengal (Prasanna Kumar et al., 1993). It is discernible from the diagram that though the arrival pattern remains same to a large extent for both the profiles, the arrivals are delayed by about 150-200 ms (milliseconds) in the presence of eddy.

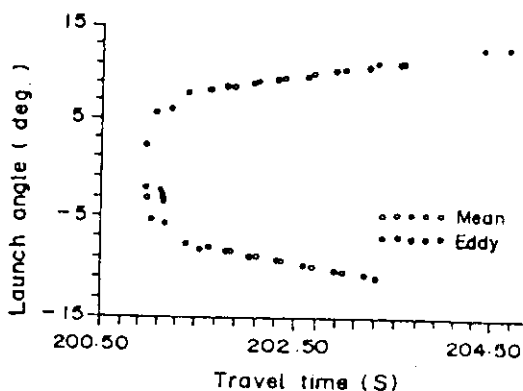


Fig.3 Travel time vs. launch angle

### ACOUSTIC INTENSITY

The intensity computed along the eigen ray (Moler and Solomon, 1970) shows that the loss associated with steep angle rays through the average field is about 70 dB while that through the eddy field is about 95 dB (Fig.4a). As the steepness of the ray decreases, the loss of intensity also decreases (Fig.4b). The flat angle rays which does not sample the eddy, undergoes intensity loss of about 80 dB in both the cases (Fig.4c). In general, the rays passing through the core/center of the eddy suffers an additional loss of intensity of the order of 20-25 dB.

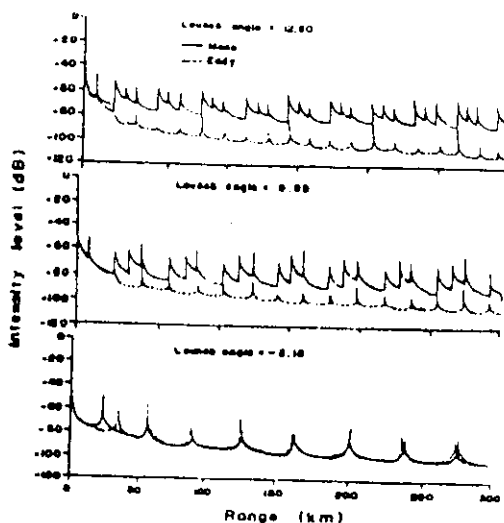


Fig.4 Acoustic intensity (dB) along the ray.

## INVERSION

In order to perform inversion of travel time data, each arrival must be associated with a particular ray path corresponding to reference as well as eddy profile. This identification is achieved by comparing the simulated arrivals for both mean and eddy in time domain (Fig.5). The inversion procedure used here is based on singular value decomposition (SVD).

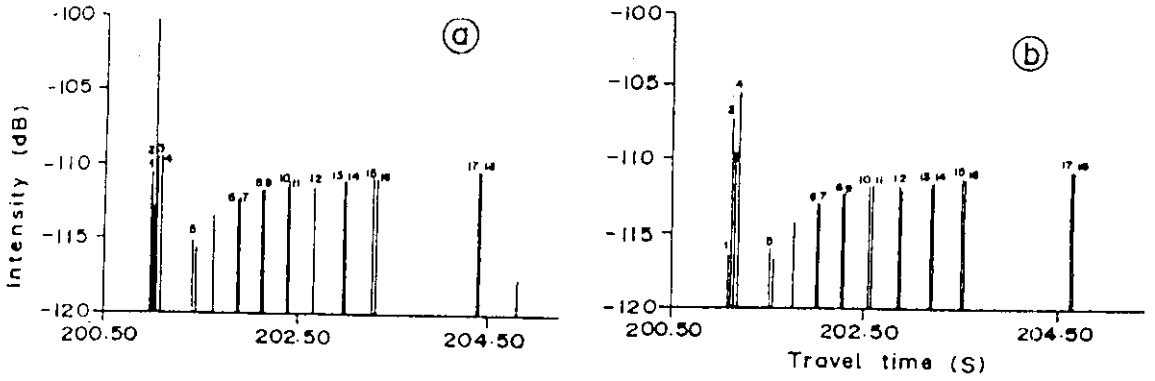


Fig. 5 Predicted travel time (a) reference & (b) eddy profile

Following Chester et al., 1991 the perturbation in travel time could be written as

$$\delta T_i = - \int \frac{\delta C(x, t)}{C_0^2(x, t_0)} ds \quad (1)$$

The model equation could be rewritten as

$$\left[ \frac{-R_{ij}}{C_0^2} \right] \delta C_j = \delta T_i \quad (2)$$

After parameterising the model, the above equation can be expressed in matrix-vector notation as

$$\delta T = A \delta C \quad (3)$$

where  $\delta T$  are the travel time differences between the measurements and those obtained by the ray model;

$A = -R_{ij}/C_0^2$  where  $R_{ij}$  is the path length of ray  $i$  in layer  $j$  and  $C_0$  is the reference sound speed. The travel time perturbation is related to sound speed perturbation through matrix  $A$ .

In the following analysis the construction of generalized

inverse operator using SVD employing eigenvalue technique has been considered (Menke, 1984). According to Jackson (1972),

the natural inverse operator  $A_g^{-1}$  always exists and is given by

$$A_g^{-1} = V \Gamma^{-1} U^T \quad (4)$$

where matrices  $V$  and  $U$  are obtained by the following coupled eigen value problem

$$A A^T U_j = \lambda_j U_j \quad (5)$$

$$A^T A V_j = \lambda_j V_j \quad (6)$$

In the above equations  $U_j$  and  $V_j$  are column vectors of matrices  $U$  and  $V$ .  $\lambda_j$  are eigen values of matrix  $A$  arranged in decreasing order. The eigen vectors corresponding to the largest eigen value indicate that large scale factors can best be determined. The selection of number of eigen values is decided by the closeness ratio approach. The solution of equation (4) is given by

$$\delta C = \left[ V \Gamma^{-1} U^T \right] \delta T \quad (7)$$

Calculations of the model resolution matrix and data resolution matrix are needed for the assessment of the resulting sound speed model.

#### Model Resolution

The model resolution of generalized inverse (5) is given by

$$R = A_g^{-1} A = V_p V_p^T$$

here  $p$  indicates number of factors used in SVD which is less than or equal to rank of the matrix  $A$ . The model parameters will be perfectly resolved if  $V_p$  spans the complete space of the model parameter i.e.

$$V_p V_p^T = I$$

#### Data Resolution

The data resolution matrix is given by

$$N = A A_g^{-1} = U_p U_p^T$$

The data are perfectly resolved if  $U_p$  spans the complete space of data. This usually tells the convergence of rays in the given domain. The SVD provides a simple frame work for determining how well the inverted model parameters fit the data and how close the model parameter estimates the true values. The larger eigen values determine the large scale features of the problem while smaller eigen values corresponds to small scale or higher frequency features.

For a number of cases using different layer depths, inversion was carried out with 18 eigen rays (Table 1). From these numerical experiments, it was found that the inversion carried out using 9 layers with layer depths 0-50, 50-100, 100-150, 150-200, 200-250, 250-1300, 1300-1800, 1800-2500, 2500-3000 gives the best result (Table.2).

Table 1. Ray identifier

	Launch angle $\theta$	Total turning + N	Upper, lower turnings (p, -p)	Travel time delay T (s)
1	2.1551	8	(4, -4)	0.1437
2	-2.1825	9	(5, -4)	0.1629
3	-5.5500	10	(5, -5)	0.1421
4	5.6262	9	(5, -4)	0.1549
5	-7.8915	12	(6, -6)	0.1531
6	-8.5651	14	(7, -7)	0.1764
7	8.4982	13	(7, -6)	0.1937
8	8.9633	14	(7, -7)	0.1952
9	-8.9910	15	(8, -7)	0.1959
10	-9.4878	16	(8, -8)	0.1963
11	9.4497	15	(8, -7)	0.2139
12	9.9555	16	(8, -8)	0.2134
13	-10.4921	18	(9, -9)	0.2130
14	10.4786	17	(9, -8)	0.2301
15	11.0177	18	(9, -9)	0.2280
16	-11.0517	19	(10, -9)	0.2283
17	-12.7616	22	(11, -11)	0.2339
18	12.8041	21	(11, -10)	0.2492

Table 2. Layer-wise sound speed perturbations

Layer depth (m)	sound speed perturbation ( $\text{m.s}^{-1}$ )	
	due to eddy	obtained through inversion
0 - 50	+0.09	+0.09
50 - 100	-7.82	-5.86
100 - 150	-12.61	-10.40
150 - 200	-8.87	-11.20
200 - 250	-4.63	-6.50
250 - 1300	-1.96	-1.56
1300 - 1800	-1.79	-1.61
1800 - 2500	-0.60	-0.38
2500 - 3000	+0.73	-0.43

For the assessment of the validity of the layering in the model used for inversion, it is essential to look at model and data resolution matrices.

Model parameter resolution is an indication of how perfectly and independently each model parameter is determined. The diagonal elements of the model parameter

resolution matrix (Fig. 6a) give a clue to how well the individual model parameters are resolved. A value of unity indicates a perfectly resolved parameter whereas a smaller value means inadequate resolution. It can be seen that 18 eigen rays and 9 layers with 9 eigen modes leads to a perfect resolution with unity diagonal elements.

The data resolution matrix is an indication of the information density of the data kernel i.e. it indicates which data contributes independent information to the solution. The diagonal elements of the data resolution matrix (Fig. 6b) shows unity in the case of box 3 and 4, indicating that the contribution of information by these middle order rays with launch angle  $-5.55^\circ$  and  $5.62^\circ$  respectively is exclusive. The low values observed in the boxes 8 to 16 indicates poor information resolution associated with higher angle rays which scans nearly same region of the water column.

VV<sup>T</sup>

0	0	0	0	0	0	0	0	1.0
0	0	0	0	.1	.2	1.0	1.0	1.0
0	0	0	0	.9	.9	1.0	1.0	1.0
0	0	0	0	0	.9	.9	1.0	1.0
0	0	0	0	0	.1	.1	1.0	1.0
.4	.8	.8	1.0	1.0	1.0	1.0	1.0	1.0
.2	.7	.8	1.0	1.0	1.0	1.0	1.0	1.0
.3	.4	.6	1.0	1.0	1.0	1.0	1.0	1.0
0	.1	.7	1.0	1.0	1.0	1.0	1.0	1.0

UU<sup>T</sup>

.1	.5	.5	.5	.5	.5	.5	.5	.5
.1	.5	.5	.5	.5	.5	.5	.5	.5
.1	.1	.8	.9	.9	1.0	1.0	1.0	1.0
.1	.1	.2	.3	.4	.9	.9	1.0	1.0
0	0	.1	.4	.4	.7	.7	.8	.8
0	.1	.1	.2	.2	.2	.2	.2	.2
.1	.1	.1	.1	.2	.2	.2	.5	.5
.1	.1	.1	.1	.1	.1	.1	.1	.1
.1	.1	.1	.1	.1	.1	.2	.2	.2
.1	.1	.1	.1	.1	.1	.2	.2	.2
.1	.1	.1	.1	.1	.1	.2	.2	.2
.1	.1	.1	.1	.1	.1	.3	.3	.3
.1	.1	.1	.1	.1	.1	.3	.3	.3
.1	.1	.1	.1	.1	.1	.3	.3	.3
.1	.1	.1	.1	.1	.1	.2	.2	.2
.1	.1	.1	.1	.2	.3	.3	.3	.3
.1	.1	.1	.2	.3	.3	.6	.6	.6

Fig.6 Diagonal elements of (a) model & (b) data resolution matrices for 9 layers and modes 1 to 9.

#### ACKNOWLEDGMENTS

The authors are thankful to Dr.B.N. Desai, Director, National Institute of Oceanography for his interest and encouragement.

#### REFERENCES

- Babu, M.T., Prasanna Kumar, S. and Rao, D.P. (1991). A subsurface cyclonic eddy in the Bay of Bengal. *Journal of Marine Research*, 49, pp 403-410.
- Chen, C. and Millero, F.J. (1977). Speed of sound in seawater at high pressures. *Journal of Acoustical Society of America*, 62, pp 1129-1135.
- Chester, D.B., Malanotte-Rizzoli, P. and De Ferrari, H. (1991). Acoustic tomography in the straits of Florida.



Journal of Geophysical Research, 96, pp 7023-7048.

Jackson, D.D. (1972). Interpretation of inaccurate, insufficient and inconsistent data. Geophysical Journal of Royal Astronomical Society, 28, pp 97-109

Menke, W. (1984). Geophysical data analysis: Discrete Inverse theory, pp 266. Academic Press, New York.

Moler, C.B. and Solomon, L.P. (1970). Use of splines and numerical integration in geometrical acoustics. Journal of Acoustical Society of America, 48, pp 739-744.

Prasanna Kumar, S., Babu, M.T. and Rao, D.P. (1992). Energy and generating mechanism of a subsurface, cold core eddy in the Bay of Bengal. Indian Journal of Marine Science, 21, pp 140-142.

Prasanna Kumar, S., Ramana Murty, T.V., Somayajulu, Y.K., Chodankar, P.V. and Murty, C.S. (1993). Reference sound speed profile and related ray acoustics of Bay of Bengal for tomographic studies. Accustica, (in press).

Ramana Murty, T.V., Somayajulu, Y.K. and Sastry, J.S. (1990). Computations of some acoustic ray parameters in the Bay of Bengal. Indian Journal of Marine Sciences, 19, pp 235-245.